NASA Technical Memorandum 83068

Surface Chemistry, Friction and Wear of Ni-Zn and Mn-Zn Ferrites in Contact With Metals

Kazuhisa Miyoshi and Donald H. Buckley
Lewis Research Center
Cleveland, Ohio

Prepared for the
Seventh Annual Conference on Composites and Advanced Ceramic Materials
sponsored by the American Ceramic Society
Cocoa Beach, Florida, January 16-20, 1983

NASA

SURFACE CHEMISTRY, FRICTION AND WEAR OF Ni-Zn AND Mn-Zn FERRITES IN CONTACT WITH METALS

Kazuhisa Miyoshi and Donald H. Buckley

National Aeronautics And Space Administration
Lewis Research Center
Cleveland, Ohio 44135

ABSTRACT

X-ray photoelectron and Auger electron spectroscopy analysis were used in sliding friction experiments. These experiments were conducted with hot-pressed polycrystalline Ni-Zn and Mn-Zn ferrites, and single-crystal Mn-Zn ferrite in contact with various transition metals at room temperature in both vacuum and argon. The results indicate that Ni_2O_3 and Fe_3O_4 were present on the Ni-Zn ferrite surface in addition to the nominal bulk constituents, while MnO_2 and Fe_3O_4 were present on the Mn-Zn ferrite surface in addition to the nominal bulk constituents. The coefficients of friction for the ferrites in contact with metals were related to the relative chemical activity of these metals. The more active the metal, the higher is the coefficient of friction. The coefficients of friction for the ferrites were correlated with the free energy of formation of the lowest metal oxide. The interfacial bond can be regarded as a chemical bond between the metal atoms and the oxygen anions in the ferrite surfaces. The adsorption of oxygen on clean metal and ferrite does strengthen the metal-ferrite contact and increase the friction. The ferrites exhibit local cracking and fracture with sliding under adhesive conditions. All the metals transferred to the surfaces of the ferrites in sliding.

INTRODUCTION

Ni-Zn and Mn-Zn mixed ferrites are ceramic semiconductors and are important as magnetic materials used for highly developed magnetic recording devices. Ni-Zn ferrite has been used for computer memory systems, such as magnetic recording disk files, while Mn-Zn ferrites have been used for video and audio tape recorders in order to enhance certain desirable properties and suppress undesirable ones in certain applications. In most magnetic recording and playback devices, recording is conducted with a magnetic head (slider) in sliding or intermittent contact with a magnetic medium, such as a magnetic tape or disk. A small amount of magnetic head and medium wear may render the recording process unreliable. The magnetic head and medium are therefore required to have good wear resistance and low friction.

Although considerable effort has been expended in determining the friction, deformation and fracture of ferrites, the friction and wear arise primarily from nonadhesive processes such as abrasion (refs. 1 to 21). Very few studies of the nature of friction and wear have been conducted with a consideration of adhesion between the sliding surfaces of ferrites (refs. 22 to 24).

The objective of the present paper is to discuss the surface chemistry, friction and wear properties of hot pressed polycrystalline Ni-Zn and Mn-Zn ferrite and single-crystal Mn-Zn ferrite in contact with various transition metals. The effects of the presence of adsorbed oxygen on the friction are also examined. The surface chemistry of the ferrite was analyzed by X-ray

photoelectron spectroscopy (XPS) and Auger electron spectroscopy (AES). Sliding friction experiments were conducted with a Ni-Zn ferrite and Mn-Zn ferrite flat specimen in contact with polycrystalline metal pins at room temperature.

All friction experiments were conducted with loads of 0.1 to 0.5 N, at a sliding velocity of 5×10^{-2} mm/s, both in a vacuum of 3x10 nPa and in argon at atmospheric pressure.

MATERIALS

The hot-pressed polycrystalline Ni-Zn ferrite and Mn-Zn ferrite were 99.9-percent-pure oxide. The porosity of the polycrystalline ferrites is less than 0.1 percent. The single-crystal Mn-Zn ferrite as grown platelets was also 99.9-percent-pure oxide. The single-crystal Mn-Zn ferrite had the (110) surface parallel to the sliding interface, and the (001) surface perpendicular to the sliding direction. The compositions and microhardness of these ferrites are shown in table I.

All the metals were polycrystalline. The titanium was 99.97 percent pure and all the other metals (Co, Cr, Fe, Ni, Re, Rh, V, W, and Zr) were 99.99 percent pure.

APPARATUSES

Two apparatuses, which basically employed a pin on a flat configuration, were used in this investigation. The details of the apparatuses are described in references 23 to 25. One apparatus, which is capable of measuring adhesion, load, and friction, was mounted in an ultrahigh vacuum system. The vacuum system contained tools for surface analysis, XPS, and AES. An ion gun was used for cleaning specimens.

The second apparatus was a system capable of measuring friction in argon (ref. 23).

EXPERIMENTAL PROCEDURES

Specimen preparation. - The sliding surfaces of the Ni-Zn and Mn-Zn ferrite flats were polished first with diamond powder approximately 3 μm and 1 μm in diameter, and with Al_2O_3 powder 1 μm in diameter. The polished surfaces had a smooth, bright, lustrous surface without evidence of any pitting.

The sliding surfaces of the polycrystalline metal pins were hemispherical and were polished first with diamond powder 3 μm and 1 μm in diameter, and then with Al_2O_3 powder 1 μm in diameter. The radius of curvature of the metal pins was 0.79 mm (1/32 in.).

Procedure. - The surfaces of the flat and pin specimens were rinsed with absolute ethanol before the experiments.

For the experiments in vacuum the specimens were placed in the vacuum chamber, and the system was evacuated and baked out to achieve a pressure of 3x10 nPa (10^{-10} torr). The flat and pin specimens were then ion sputter cleaned.

Ion sputter etching was performed with a beam energy of 3000 eV at 20-mA beam current with an argon pressure of 7×10^{-4} Pa. The ion beam was continuously rastered over the specimen surface. After sputter etching, the system was re-evacuated to a pressure of 3x10 nPa or lower. The surface cleanliness was verified by XPS or AES analysis.

In-site friction experiments were conducted with the sputter cleaned ferrite flat and metal pin specimens. A load of 0.1 to 0.5 N was applied to the pin-flat contact. To obtain consistent experimental conditions, the time in contact before sliding was 30 s. Both load and friction forces were continuously monitored during a friction experiment. Sliding velocity was 5×10^{-2} mm/s with a total sliding distance of 2 to 3 mm. The values of coefficients of friction reported herein were obtained by averaging three to five measurements. The standard deviation of the measured values are within 4 percent of the mean value.

In those experiments designed to examine the adsorbed oxygen effect on friction, atomically sputter cleaned ferrite and metal surfaces were exposed to 1000 L (L = 1×10^{-6} torr · s) of O_2 with an oxygen pressure of 1×10^{-6} torr.

At completion of the exposure, the vacuum system was re-evacuated to a pressure of 3x10 nPa or lower. The surface chemistry of the specimens was examined by XPS analysis. Friction experiments were conducted with the ferrites and metal specimens, which were exposed to oxygen, in the same manner as with atomically clean specimens.

In the argon atmosphere, the specimens were placed into the second experimental apparatus. The pin and flat specimen surfaces were then brought into contact and loaded by deadweights and the friction experiment was initiated.

RESULTS AND DISCUSSION

Surface Chemistry

Ni-Zn ferrite. - The XPS survey spectra of Ni-Zn ferrite surfaces obtained before sputter cleaning revealed primarily oxygen and carbon contamination peaks, as shown in figure 1(a). An XPS spectrum of the ferrite surface after sputter cleaning for 20 min is shown in figure 1(b). The carbon contamination peak has nearly disappeared from the spectrum. In addition to oxygen and iron, the XPS peaks indicate nickel and zinc on the surface.

The XPS spectra of Ni_{2p}, Zn_{2p}, Fe_{2p} and O_{1s} obtained from narrow scans on the Ni-Zn ferrite surfaces are presented in figure 2.

The $Ni_{2p3/2}$ photoelectron emission lines of the Ni-Zn ferrite after argon sputter cleaning are primarily split asymmetrically into doublet peaks. They are peaked at 853.3 and 855.0 eV. It is interesting in that the binding energies of the doublet peaks match both $NiFe_2O_4$ (or Ni^{2+} ion in NiO) and Ni_2O_3, respectively (refs. 26 and 27).

The Zn_{2p} photoelectron lines for the Ni-Zn ferrite peaked primarily at 1021.7 eV, which is associated with ZnO.

The $Fe_{2p3/2}$ photoelectron lines peaked primarily at 710.8 eV. The binding energy matches that for both Fe_2O_3 and $NiFe_2O_4$, which are extremely close in energy and difficult to distinguish in the data of figure 2(c). Fe_{2p} peak associated with Fe_3O_4 is also observed on the surface. In figure 2(d), in addition to the adsorbed oxygen contamination peaks, the O_{1s} peak associated with Fe_2O_3 is observed on the as-received Ni-Zn ferrite surface. The peak intensity at 530 eV associated with Fe_2O_3 increased with an increase in sputtering time up to 20 min.

Table II summarizes various constituents present on the Ni-Zn ferrite surface and their relative concentrations before and after sputtering.

The relative concentrations of adventitious hydrocarbon, present on the as-received Ni-Zn ferrite and introduced from the specimen preparation process, were about 79 at.%. After sputtering almost no carbon was evident on the Ni-Zn ferrite surface.

The concentrations of nickel oxides (NiO and Ni_2O_3), ZnO and Fe_2O_3 on the Ni-Zn ferrite obtained from the XPS spectra are interesting in that the concentration of ZnO is less than that of nickel oxides on the surface, while the concentration of ZnO in the bulk is greater than that of nickel oxides, as shown in table II. The results suggest that Zinc may segregate and be sputtered away from the surface during argon ion sputtering.

Mn-Zn ferrite. - The XPS survey spectra of the Mn-Zn ferrite surfaces obtained before sputter cleaning revealed primarily oxygen and carbon contamination peaks, as shown in figure 3(a). An XPS spectrum of the ferrite surface after sputter cleaning for 20 min is also shown in figure 3(b). The carbon contamination peak has nearly disappeared from the spectrum. In addition to oxygen and iron, the XPS peaks clearly indicate manganese and zinc on the surface.

Figure 4 presents the XPS spectra of Mn_{2p}, Zn_{2p}, Fe_{2p} and O_{1s} obtained from narrow scans on the Mn-Zn ferrite surfaces.

The $Mn_{2p3/2}$ photoelectron emission lines of the Mn-Zn ferrite after cleaning include two peaks. The binding energies of the peaks match both MnO and Mn^{2+} ion in the MnO_2 (ref. 26).

The Zn_{2p} photoelectron lines for the Mn-Zn ferrite peaked primarily at 1021.7 eV, which is associated with ZnO. The $Fe_{2p3/2}$ photoelectron lines primarily include Fe_2O_3 as well as a small amount of Fe_3O_4, as shown in figure 4.

The O_{1s} peaks obtained from the as-received surface are associated with the adsorbed oxygen contamination and Fe_2O_3. After sputtering the XPS peaks indicate Fe_2O_3 on the Mn-Zn ferrite surface.

Table III summarizes various constituents present on the Mn-Zn ferrite surface and their relative concentrations before and after sputtering.

The relative concentrations of hydrocarbon contaminant was about 71 at. %. After sputtering no carbon is evident on the Mn-Zn ferrite surface. The concentration of ZnO is less than that of manganese oxides on the surface, while the concentration of ZnO in the bulk is greater than that of manganese oxides. This result is consistent with that of Ni-Zn ferrite chemistry, already mentioned.

Friction Behavior and Environmental Effects

Sliding friction experiments were conducted with Ni-Zn and Mn-Zn ferrites in contact with various metals both in vacuum and in argon at atmospheric pressure. Typical results are presented in figure 5. The marked difference in friction for the two environments shows the effects of adsorbate and environment on the friction properties. The results in ultrahigh vacuum are to be anticipated from chemical interactions and the important role they play in the friction of ferrite-metal couples. This subject is explained in detail in the following section. The coefficients of friction for various metals sliding on Ni-Zn and Mn-Zn ferrite in argon atmosphere were all approximately 0.1 to 0.2. The chemical activity or inactivity of a metal does not appear to play a role in the friction in argon. A prerequisite for this sameness in friction is that the metals form a stable metal oxide and the environment provide adsorbates formed on the surfaces. The oxides of the metal in figure 5 are all very stable. Note that the coefficients of friction for various metals sliding on the ferrites in vacuum and in argon were unaffected by load in the range of 0.1 to 0.5 N.

Effect of Metal Activity on Friction

The relative chemical activity of the transition metals (metals with partially filled d shells) as a group can be ascertained from their percentage d bond character, as shown by Pauling (ref. 28). The frictional properties of metal-metal and metal-ceramic contacts have been shown to be related to this character (refs. 29 to 32 and 22). The greater the percentage of d bond character, the less active is the metal and the lower is the friction. Conversely, the more active the metal, the higher is the coefficient of friction.

The coefficients of friction for various metals in contact with the hot-pressed polycrystalline Ni-Zn and Mn-Zn ferrites are presented in figure 6 as a function of the d bond character of the transition metal. Titanium, which is a chemically active metal, exhibits a considerably higher coefficient of friction in contact with ferrite than does rhodium, which is a metal of lesser activity. This result is consistent with the authors' earlier studies conducted with single-crystals of SiC, diamond, and single-crystal Mn-Zn ferrite (refs. 22, 30, and 32).

In figure 6(b), the coefficients of friction with single-crystal Mn-Zn ferrite are lower than those of the hot-pressed polycrystalline Mn-Zn ferrite. This difference in friction may be in accord with effects of crystallographic orientation and grain boundary as well as impurities contained in the crystals. The crystallographic plane and direction can play a significant role in the friction behavior of ferrites (refs. 22 and 24). Sliding along the direction which is most closely packed minimizes the adhesion and friction.

The coefficients of friction can also be correlated with the free energy of formation of the lowest metal oxides, as shown in figure 7. This correlation is consistent with the results of Pepper (ref. 33); that is, the shear coefficients of the clean metal (Ag, Cu, Ni, and Fe)-to-sapphire contacts correlate with the free energy of formation of the lowest metal oxide.

The correlation shown in figure 7 clearly indicates that the metal-ferrite bond at the interface is primarily a chemical bond between the metal atoms and the large oxygen anions in the ferrite surface and the strength of this bond is related to the oxygen-metal bond strength in the metal oxide (refs. 33 to 37).

Note that all the metals shown in figure 7 transferred to the surfaces of the ferrites. In general the less active the metal, the less transfer to the ferrite. Titanium, having a much stronger chemical affinity to the elements of the ferrite, exhibited the greatest amount of transfer (refs. 22 and 23).

Effect of Oxygen Adsorption on Friction

Figure 8 presents the coefficients of friction for various metals in contact with the ferrites, in which both metal and ferrite specimens were exposed to O_2 gas. The data of figure 8 indicate the coefficients of friction as a function of the d-bond character of the metal. The data reveal a decrease in friction with an increase in d-bond character. The adsorption of oxygen on argon sputter cleaned metal and ferrite surfaces produces two effects: (1) the metal oxidizes and forms an oxide surface layer; and (2) the oxide layer increases the coefficients of friction for both Ni-Zn ferrite-to-metal and Mn-Zn ferrite-to-metal interfaces.

The oxygen exposures did strengthen the metal-to-ferrite adhesion and increased the friction. The enhanced bond of the metal oxide to ferrite may be due to the formation of complex oxides on establishing contact.

Fracture Wear of Ferrites

The sliding of a metal pin on Ni-Zn and Mn-Zn ferrite surfaces results in the formation of cracks and fracture pits in the ferrite surfaces as well as metal wear and metal transfer to the ferrite surfaces both in vacuum and argon. The coefficient of friction was greater and fracture of ferrite and metal wear was larger in vacuum than it was in argon.

The removal of adsorbed films (usually water vapor, carbon monoxide, carbon dioxide and oxide layers) from the surfaces of metals and ferrites results in very strong interfacial adhesion when two solids are brought into contact. The adhesive bonds formed at the metal-to-ferrite interface are sufficiently strong that fracture of the cohesive bonds in the metal and transfer of the metal to the ferrite surfaces results. All the metals used in this investigation transferred to the ferrites. This fracture wear of the ferrites occurs very locally and in very small areas in and near the sliding contact region.

Figures 9 and 10 are scanning electron micrographs of wear tracks on single-crystal and polycrystalliane Mn-Zn ferrite. In figure 9, three types of cracking in the wear track are observed: One type is characterized by a small crack propogating perpendicular to the sliding direction. It propagates below the surface from the high compressive stress at the real contact area of the pin during sliding. The second type is a crack propagating at an inclination of about 45° to the sliding direction, that is, along cleavage planes of {110}. The third type obtained is a crack propagating parallel to the sliding direction, that is, also along the cleavage planes of {110}.

Figure 10 reveals that the extent of small cracking in polycrystalline Mn-Zn ferrite depends on the orientation of the individual crystallites and the direction of sliding. It is obvious that a significant degree of cracking begins in a grain boundary and extends along the grain boundaries. The fracturing of the polycrystalline ferrite surface is the result of cracks propagating and intersecting other cracks in grain boundaries. The cracks and fracture can originate from a void, as these are primarily in grain boundaries.

The wear scar on the metal pin after it slid against ferrites revealed evidence of a large number of plastically deformed grooves, as typically shown in figure 11. Figure 11 presents scanning electron micrographs of the pin wear scar on titanium resulting from five passes of the titanium pin over the Mn-Zn ferrite surface in vacuum.

The wear scar on metals after sliding on ferrite surfaces may occasionally contain small amounts of wear debris generated by the fracture of ferrite surfaces and the transfer of the debris to the metal surfaces, as typical shown in figure 12. Figure 12 clearly reveals that the wear debris of ferrite was embedded in the metal surface.

CONCLUSIONS

As a result of the XPS and AES analysis and the sliding friction experiments conducted with Ni-zn and Mn-zn ferrite surfaces in sliding contact with various transition metals in a vacuum and in argon, the following conclusions are drawn.

1. Ni_2O_3 and Fe_3O_4 are present on the Ni-Zn ferrite surface in addition to the normal constituents such as NiO ($NiFe_2O_4$), ZnO and Fe_2O_3. MnO_2 and Fe_3O_4 were present on the Mn-Zn ferrite surface in addition to the normal constituents such as MnO, ZnO and Fe_2O_3.

2. The coefficients of friction for Ni-Zn and Mn-Zn ferrites in contact with various metals were related to the relative chemical activity of these metals. The more active the metal, the higher is the coefficient of friction. They were also correlated with the free energy of formation of the lowest metal oxide. The interfacial bond can be regarded as a chemical bond between the metal atoms and the oxygen anions in the ferrite surfaces.

3. The adsorption of oxygen on clean metal and ferrite does strengthen the metal-ferrite contact and increase the friction. The enhanced bond of the metal oxide to ferrite may be due to the formation of the complex oxides on establishing contacts.

4. The ferrites exhibit very local cracking and fracture with sliding under adhesive conditions. All metals transferred to the surfaces of the ferrites in sliding.

REFERENCES

1. K. Tanaka, K. Miyoshi, H Araki and T. Murayama, "Friction and Wear in the Sliding of VTR Head Against Magnetic Tape. (1st rpt.) - Contact Force and Frictional Force," J. Jpn. Soc. Precis. Eng., 40 [7], 550-556 (1974).
2. K. Tanaka, K. Miyoshi, H. Araki and T. Murayama, "Friction and Wear in the Sliding of VTR Head Against Magnetic Tape. (2nd rpt.) - Wear of VTR Head Made of a Ferrite Single Crystal, "J. Jpn. Soc. Precis. Eng., 40 [8] 651-657 (1974).
3. K. Tanaka, K. Miyoshi and T. Murayama, "Friction and Wear in the Sliding of VTR Head Against Magnetic Tape (3rd rpt.) - Effect of Wear on the Output Signal Level", J. Jpn. Soc. Precis. Eng., 40 [9] 785-792 (1974).
4. K. Tanaka and K. Miyoshi, "Friction and Wear of Magnetic Tape. Part I Frictional Behavior," J. Jpn. Soc. Lubr. Eng., 19, [9] 645-653 (1974).
5. K. Tanaka, K. Miyoshi, M. Tsunekawa and T. Murayama, "Friction and Deformation of Mn-Zn Ferrite Single Crystals. (1st rpt.) - Contact and Friction of Ferrite Single Crystals," J. Jpn. Soc. Precis. Eng., 41 [2] 148-154 (1975).
6. K. Tanaka, K. Miyoshi and T. Murayama, "Friction and Deformation of Mn-Zn Ferrite Single Crystals - Frictional Properties and Deformation," Bull. Jpn. Soc. Precis. Eng., 9 [1] 27-34 (1975).
7. K. Tanaka, K. Miyoshi and T. Murayama, "Friction and Deformation of Mn-Zn Ferrite Single Crystals - Crack Formation," Bull. Jpn. Soc. Precis. Eng., 9 [2] 47-48 (1975).
8. K. Tanaka, K. Miyoshi, T. Hirose and T. Murayama, "Abrasive Wear of Mn-Zn Ferrite. (1st rpt.) Effects of Abrasive Grain Size and Contact Pressure. J. Jpn. Soc. Precis. Eng., 41 [9] 896-902 (1975).

9. K. Tanaka, K. Miyoshi, Y. Miyao and T. Murayama, "Friction and Deformation of Mn-Zn Ferrite Single Crystals," pp. 58-66 in Proceeding of JSLE-ASLE International Lubrication Conference, Tokyo, 1976. Edited by T. Sakurai. Elsevier Scientific Publishing Co., 1976.
10. K. Miyoshi, K. Tanaka and T. Murayama. "Friction and Wear of Magnetic Tape. Part 2 Effects of Surface Roughness of Countersurface on Friction, "J. Jpn. Soc. Lubr. Eng., 21 [11] 756-763 (1976).
11. K. Miyoshi, K. Tanaka and T. Murayama, "Abrasive Wear of Mn-Zn Ferrite. (2nd rpt.) Effects of Sliding Speed and Abrasive/Carrier Fluid Ratio," J. Jpn. Soc. Precis. Eng., 43 [4] 483-488 (1977).
12. K. Miyoshi, K. Tanaka and T. Murayama, "Abrasive Wear of Mn-Zn Ferrite. (3rd rpt.) Deformed Crystalline Layers and Surface Cracking." J. Jpn. Soc. Precis. Eng., 43 [10] 1192-1197 (1977).
13. K. Miyoshi, K. Tanaka, Y. Fuwa and T. Murayama, Tape Lapping of Manganese - Zinc Ferrite Crystals. (1st rpt) Frictional Properties and Abrasiveness of Lapping Tapes. J. Jpn. Soc. Precis. Eng., 43 [23] 1395-1401 (1977).
14. J. F. Carroll, Jr., and R. C. Gotham, "The Measurement of Abrasiveness of Magnetic Tape," IEEE Trans. Magn., mag-2 [2] 6-13 (1966).
15. F. E. Talke, and J. L. "The Mechanism of Wear in Magnetic Recording Disk Files," Tribol. Int., 8 [1] 15-20 (1975).
16. W. D. Kehr, C. B. Meldrum, and R.F.M. Thornley, "The Influence of Grain Size on the Wear of Nickel-Zinc Ferrite by Flexible Media, "Wear, 31, 109-117 (1975).
17. K. Tanaka, and O. Miyazaki, "Wear of Magnetic Materials and Audio Heads Sliding Against Magnetic Tape," Wear, 66, 289-306 (1981).
18. F. W. Hahn, Jr. "Materials Selection for Digital Recording Heads," pp. 199-203 in Proceedings of Wear Materials. The International Conference on Wear of Materials, St. Louis, Missouri, 1977. Edited by W.A. Glaeser, K.C. Ludema and S.K. Rose. ASME, 1977..
19. A. Begelinger, and A. W. J. deGee, "Wear Measurements using Knoop Diamond Indentions," wear, 43, 259-261 (1979).
20. A. B. Van Groenou, N. Maan, and J.O.B. Veldkamp, "Scratching Experiments on Various Ceramic Materials," Philips Res. Rep., 30 [5] 320-359 (1975).
21. K. Miyoshi, "Lapping of Manganese-Zinc Ferrite by Abrasive Tape," Lubr. Eng., 38 [3] 165-172 (1982).
22. K. Miyoshi, and D. H. Buckley, "Friction and Wear of Single-Crystal Manganese-Zinc Ferrite," Wear, 66, 157-173 (1981).
23. K. Miyoshi, and D. H. Buckley, "Friction and Wear of Single-Crystal and Polycrystalline Manganese-Zinc Ferrite in Contact with Various Metals," NASA TP 1059, 1977.
24. K. Miyoshi, and D. H. Buckley, "Anisotropic Friction and Wear of Single-Crystal Manganese-Zinc Ferrite in Contact with Itself, "NASA TP-1339, 1978.
25. K. Miyoshi, D. H. Buckley, and Srinivasan "Tribological Properties of Sintered Polycrystalline and Single-Crystal Silicon Carbide," Amer. Cer. Soc. Bull., in process.
26. C. D. Wagner, W. M. Riggs, L. E. Davis, J. F. Moulder, and G.E. Muilenberg, Handbook of X-ray Photoelectron Spectroscopy. Perkin-Elmer, Physical Electronics Division, Eden Prairie, Minnesota, 1978.

27. G. C. Allen, P. M. Tucker, and R. K. Wild, "Surface Oxidation of Nickel Metal as Studied by X-ray Photoelectron Spectroscopy," Oxid. Met. 13 [3] 223-236 (1979).
28. L. Pauling, "A Resonating-Valence-Bond Theory of Metals and Intermetallic Compounds," Proc. Roy. Soc. (London), ser. A, 196 [1046,] 343-362 (1949).
29. D. H. Buckley, "The Metal-to-Metal Interface and Its Effect on Adhesion and Friction," J. Colloid Interface Sci., 53 [2], 36-53 (1977).
30. K. Miyoshi, K. and D. H. Buckley, "Adhesion and Friction of Single-Crystal Diamond in Contact with Transition Metals, "Appl. Sur. Sci., 6, 161-172 (1980).
31. D. H. Buckley, "Friction and Transfer Behavior of Pyrolytic Boron Nitride in Contact with Various Metals," ASLE Trans., 21 [2], 118-124 (1978).
32. K. Miyoshi, and D. H. Buckley, "Friction and Wear Behavior of Single-Crystal Silicon Carbide in Sliding Contact with Various Metals," ASLE Trans., 22, [3] 245-256 (1979).
33. S. V. Pepper, "Shear Strength of Metal-Sapphire Contacts," J. App. Phys. 47 [3] 801-808 (1976) .
34. C. R. Kurkjian, and W. D. Kingery, "Surface Tension at Elevated Temperatures. III. Effect of Cr, In, Sn, and Ti on Liquid Nickel Surface Tension and Interfacial Energy with Al_2O_3," J. Phys. Chem., 60, 961-963 (1956).
35. J. E. McDonald, and J. G. Eberhart, Adhesion in Aluminum Oxide-Metal Systems," AIME Trans., 233, 512-517 (1965).
36. C. J. Smithells, Metals Reference Book. (Vol. 1). Plenum, New York, 1967.
37. A. Glassner, "The Thermochemical Properties of the Oxides, Fluorides, and Chlorides to 2500° K." Argonne National Laboratory, ANL-5750, 1957.

TABLE I. - COMPOSITION AND HARDNESS DATA ON Ni-Zn and Mn-Zn FERRITES

(a) Hot-pressed polycrystalline Ni-Zn ferrite

Composition, at. %	Fe_2O_3	66.6
	NiO	11.1
	ZnO	22.2
Grain size, μm		8
Porosity, percent		<0.1
Vickers hardness[a]		715

(b) Hot-pressed polycrystalline Mn-Zn ferrite

Composition, at. %	Fe_2O_3	69.1
	MnO	15.2
	ZnO	15.7
Grain size, μm		24
Porosity, percent		<0.1
Vickers hardness[a]		640

(c) Single-crystal Mn-Zn ferrite

Composition, at. %	Fe_2O_3	71.6
	MnO	17.3
	ZnO	11.1
Sliding surface		(110)
Sliding direction		<001>
Knoop hardness[b]		560
Vickers hardness[a]		645

[a]Knoop hardness measuring load was 3 N.
[b]Vickers hardness measuring load was 0.5 N.

TABLE II. - VARIOUS CONSTITUENTS ON THE Ni-Zn FERRITE AND THEIR CONCENTRATION

(a) Elements

Surface treatment in vacuum chamber	Concentration, at. %				
	Ni	Zn	Fe	O	C
No treatment	1	1	3	16	79
Sputtering	9	5	30	56	--

(b) Oxides

Surface treatment in vacuum chamber		Concentration, mol %		
		NiO (Ni_2O_3)	ZnO	Fe_2O_3 (Fe_3O_4)
Surface:	No treatment	17	17	66
	Sputtering	20	10	70
Bulk		11.5	20.0	68.4

TABLE III. - VARIOUS CONSTITUENTS ON THE Mn-Zn FERRITE AND THEIR CONCENTRATION

(a) Elements

Surface treatment in vacuum chamber	Concentration, at. %				
	Mn	Zn	Fe	O	C
No treatment	3	1	4	21	71
Sputtering	11	3	29	57	--

(b) Oxides

Surface treatment in vacuum chamber		Concentration, mol %		
		MnO (MnO_2)	ZnO	Fe_2O_3 (Fe_3O_4)
Surface	No treatment	36	15	49
	Sputtering	26	7	67
Bulk		15.7	14.1	70.2

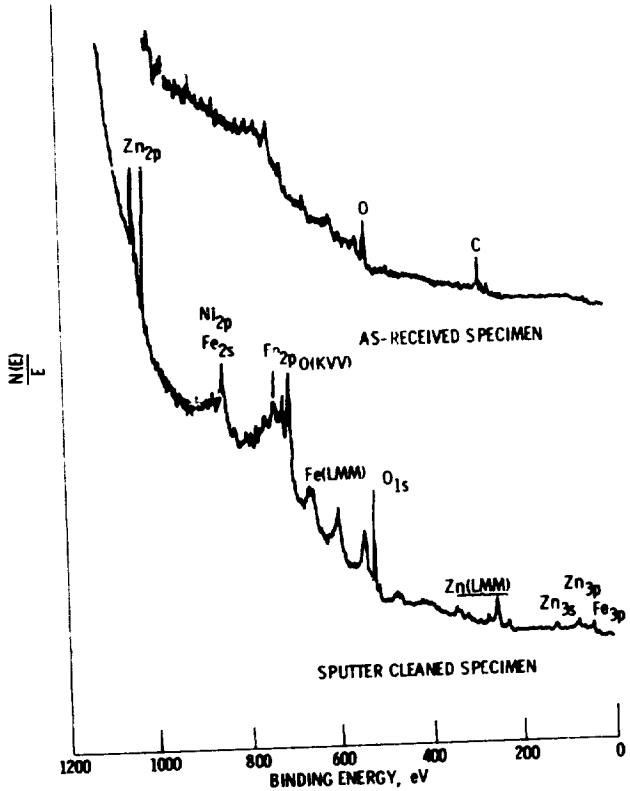

Figure 1. - XPS survey spectra of the Ni-Zn ferrite surfaces.

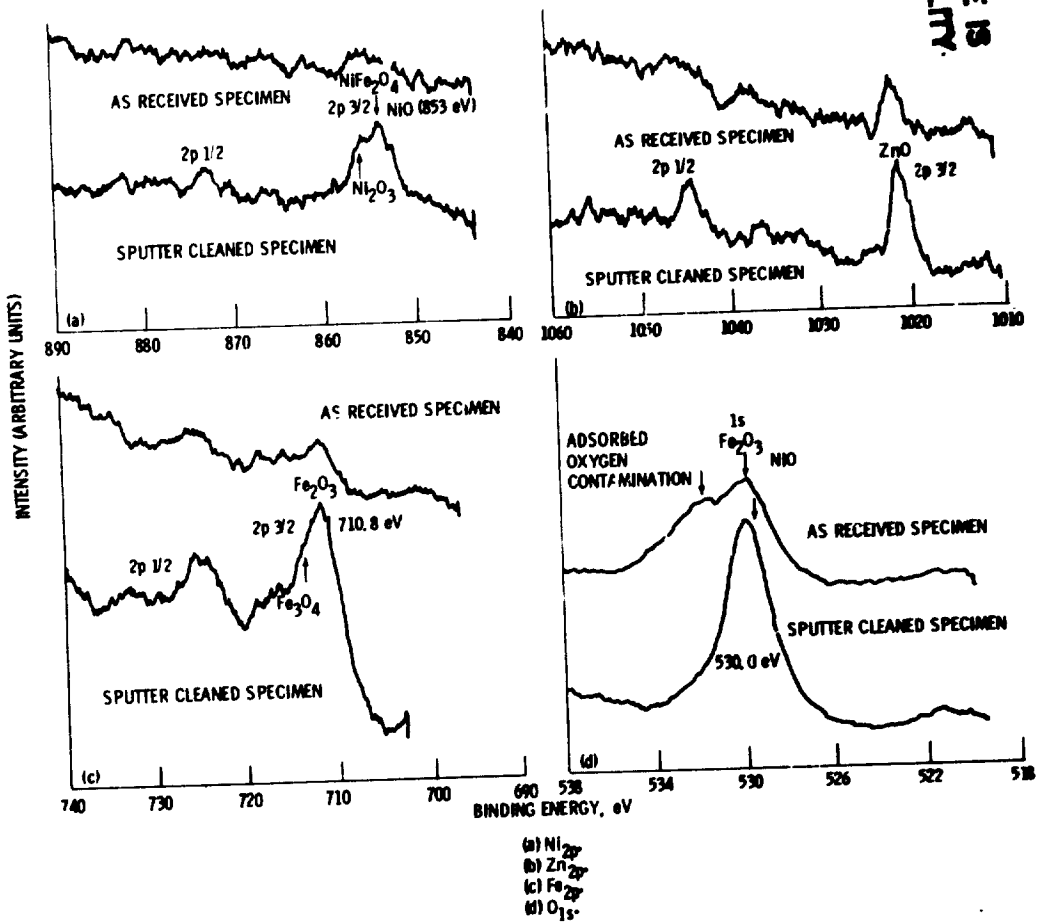

(a) Ni_{2p}
(b) Zn_{2p}
(c) Fe_{2p}
(d) O_{1s}.

Figure 2. - Ni_{2p}, Zn_{2p}, Fe_{2p}, and O_{1s} XPS peaks on Ni-Zn ferrite surfaces.

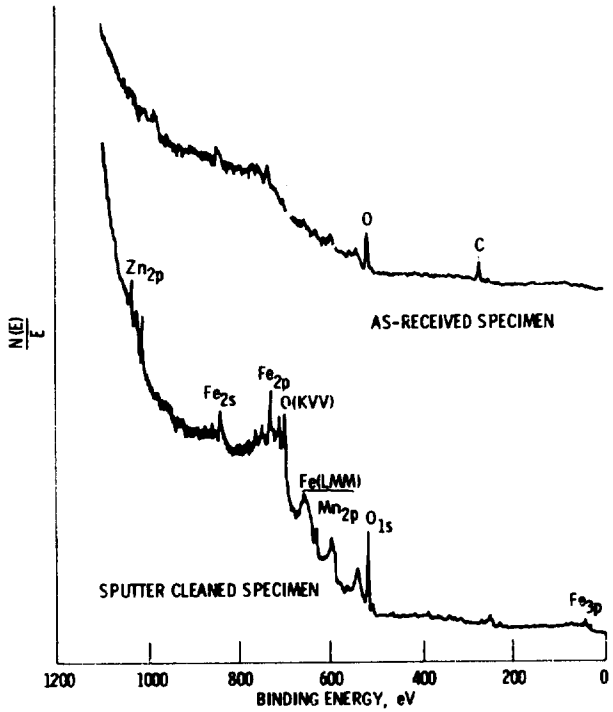

Figure 3. - XPS survey spectra of the Mn-Zn ferrite surfaces.

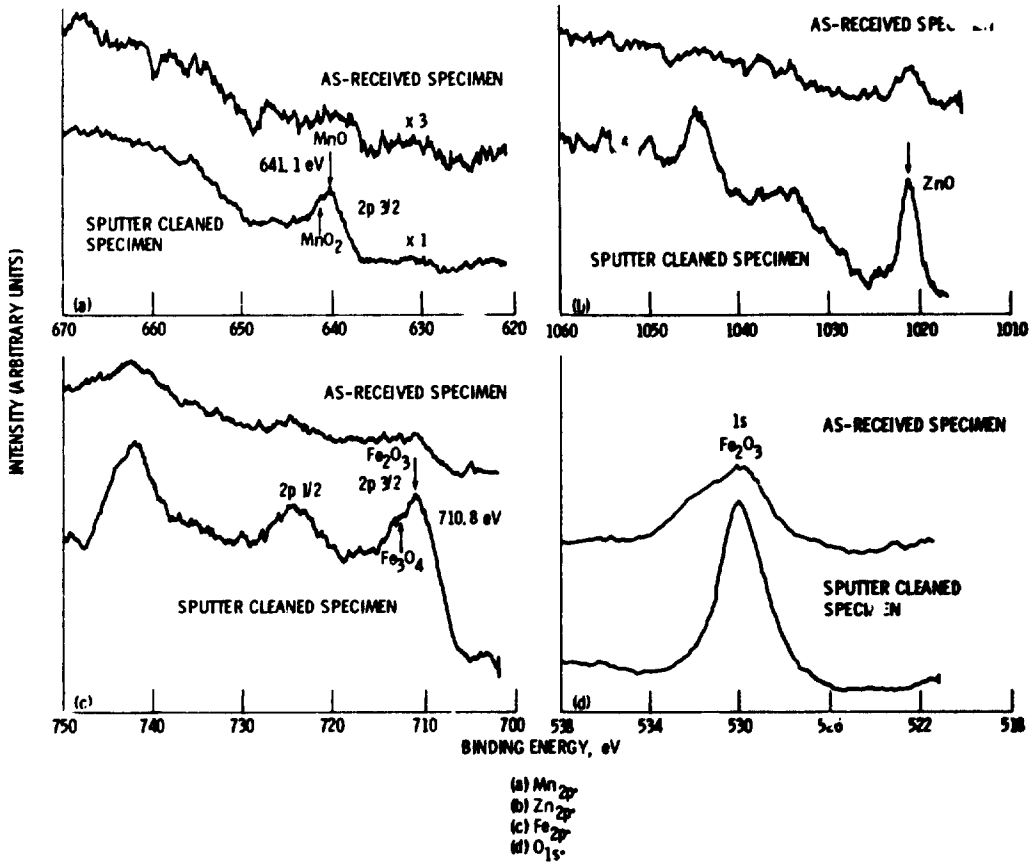

(a) Mn_{2p}
(b) Zn_{2p}
(c) Fe_{2p}
(d) O_{1s}.

Figure 4. - Mn_{2p}, Zn_{2p}, Fe_{2p}, and O_{1s} XPS peaks on Mn-Zn ferrite surfaces.

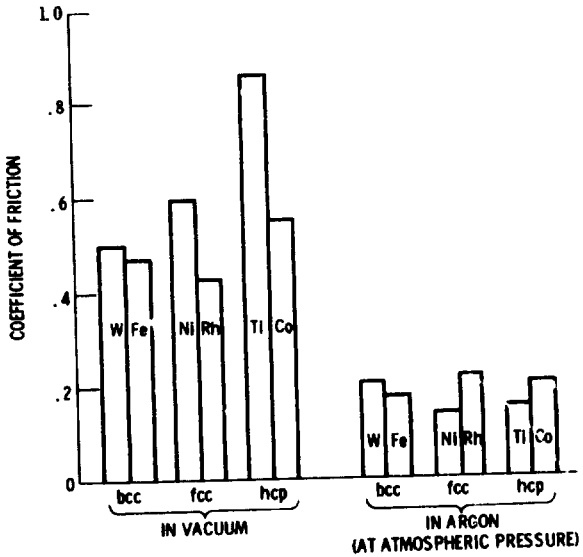

Figure 5. - Coefficient of friction as function of percent of d bond character of various metals in sliding contact with Mn-Zn ferrite (110) surface in vacuum (3x10 nPa) and in argon at atmospheric pressure. Sliding velocity, 3 mm/min; load, 0.05 to 0.5 N; room temperature.

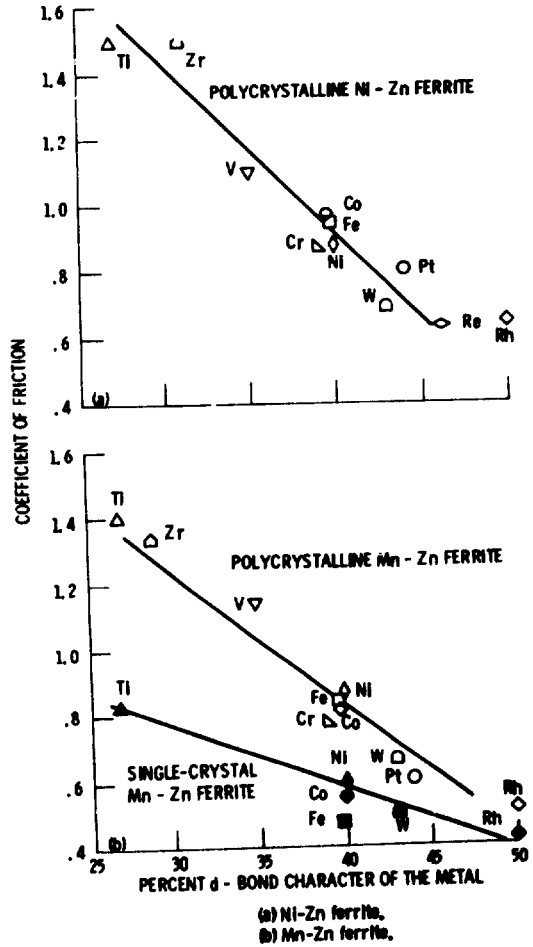

(a) Ni-Zn ferrite.
(b) Mn-Zn ferrite.

Figure 6. - Coefficient of friction as a function of the percentage d bond character of various metals in sliding contact with Ni-Zn and Mn-Zn ferrites in vacuum (3x10 nPa). Single pass sliding; sliding velocity, 3 mm/min; load, 0.05 to 0.2 N; room temperature.

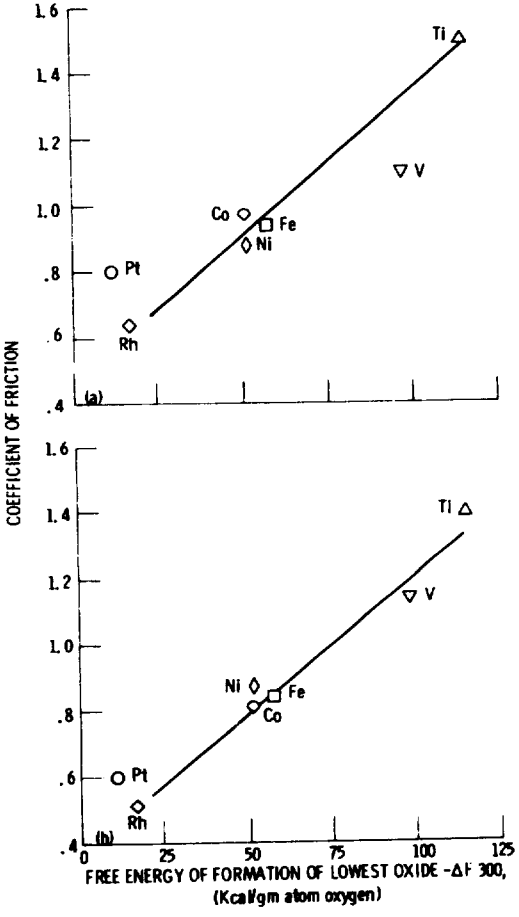

(a) Ni-Zn ferrite.
(b) Mn-Zn ferrite.

Figure 7. - Coefficients of friction for various metals in contact with the ferrites as a function of the free energy of formation of lowest oxide. Single pass sliding; sliding velocity, 3 mm/min; load, 0.05 to 0.2 N; vacuum, 3x10 nPa; room temperature.

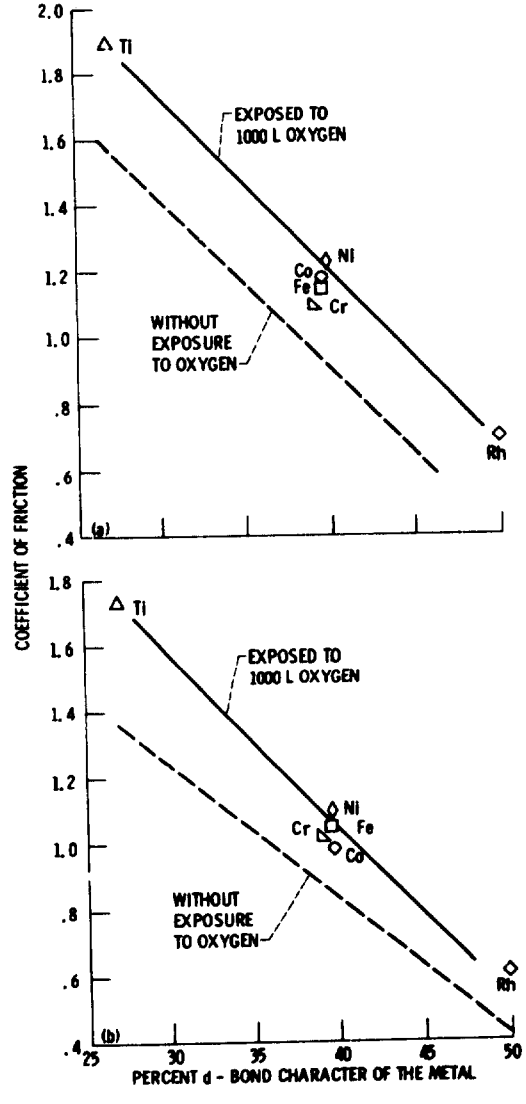

(a) Ni-Zn ferrite.
(b) Mn-Zn ferrite.

Figure 8. - Effect of adsorbed oxygen on friction for various metals in contact with the ferrites. Exposure, 1000 L in oxygen gas; sliding velocity, 3 mm/min; load, 0.05 to 0.2 N; vacuum, 3x10 nPa; room temperature.

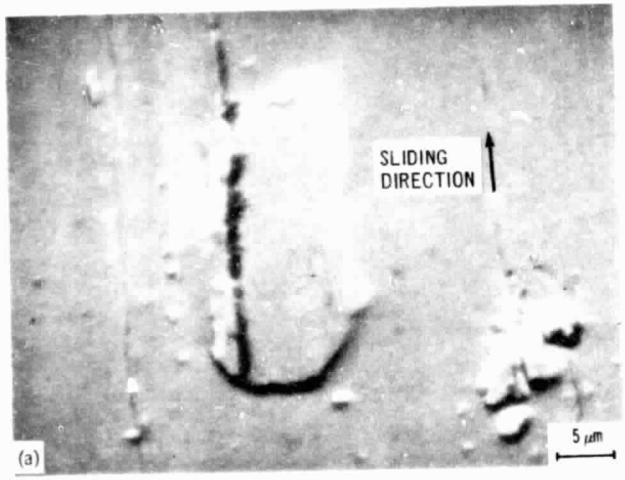

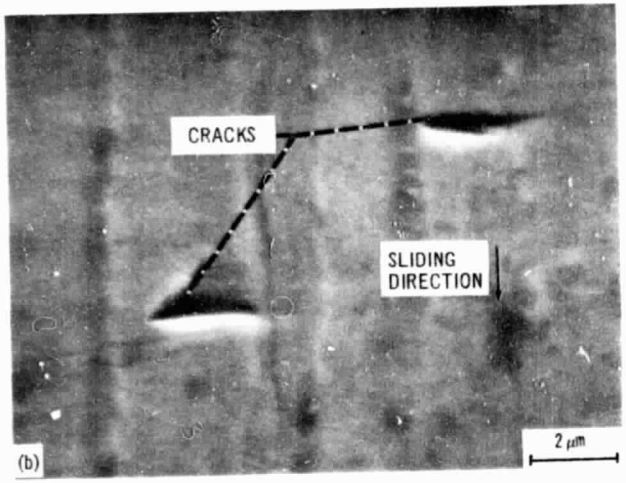

(a) CRACKS PROPAGATING PERPENDICULAR TO, PARALLEL TO, AND AT AN INCLINATION OF ABOUT 45° TO SLIDING DIRECTION.

(b) CRACKS PROPAGATING PERPENDICULAR TO AND AT AN INCLINATION OF 45° TO SLIDING DIRECTION.

Figure 9. - Scanning electron micrographs of wear track and cracking of single-crystal manganese-zinc ferrite (110) surface after five passes of cobalt rider in high vacuum (10^{-8} N/m^2). Sliding velocity, 3 mm/min; temperature, 25° C.

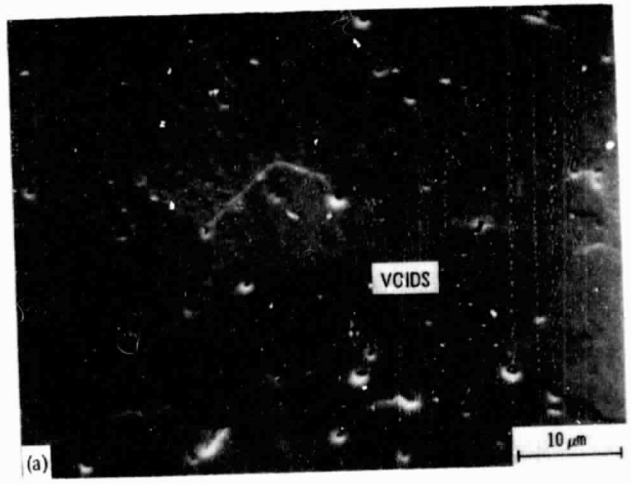

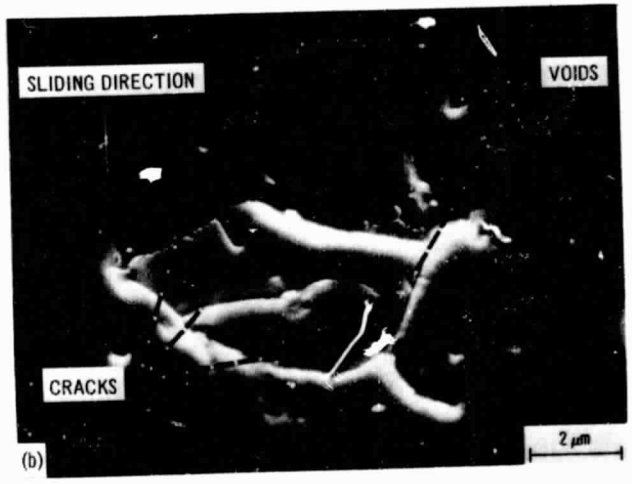

(a) MICROSTRUCTURE OF HPF (ETCHED) BEFORE SLIDING OF RHODIUM RIDER.

(b) CRACKING AROUND GRAIN.

Figure 10. - Scanning electron micrographs of wear track and cracking of hot-pressed polycrystalline manganese-zinc ferrite surface (etched) after five passes of rhodium rider in high vacuum (10^{-8} N/m^2). Sliding velocity, 3 mm/min; temperature, 25° C.

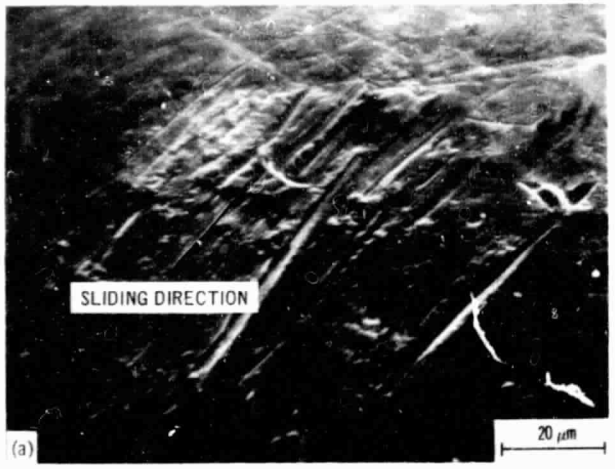

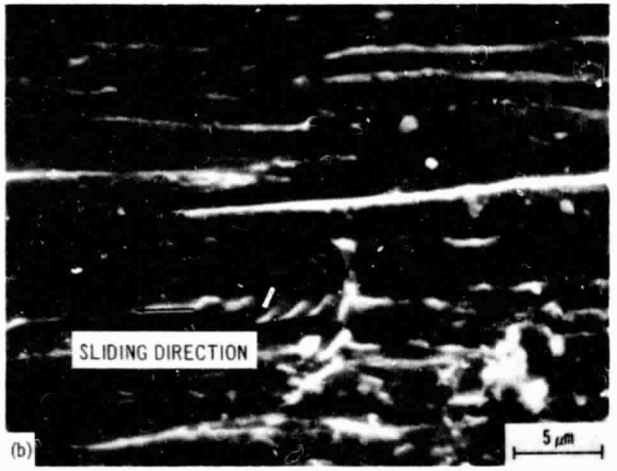

(a) WEAR SCAR AS RESULT OF FIVE PASSES.

(b) PLASTICALLY DEFORMED GROOVES.

Figure 11. - Scanning electron micrographs of wear scar on titanium rider after sliding on single-crystal manganese-zinc ferrite (110) surface in high vacuum (10^{-8} N/m^2). Sliding velocity, 3 mm/min; load, 30 grams; temperature, 25° C.

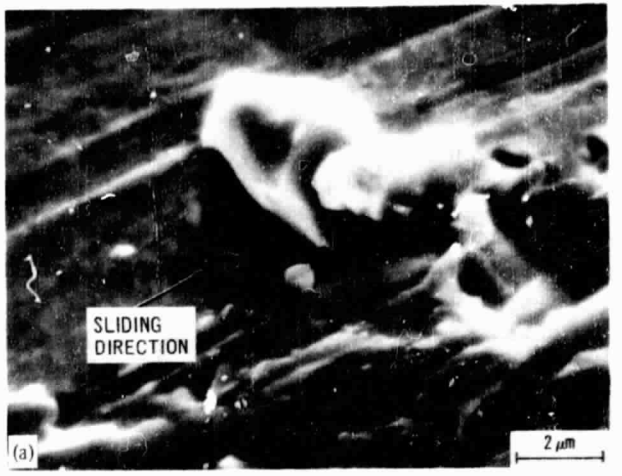

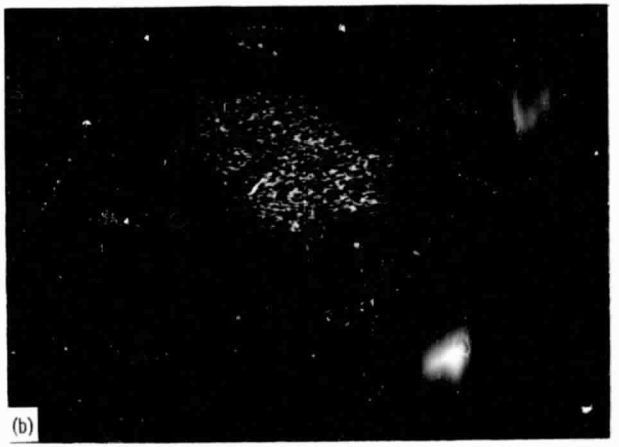

(a) WEAR DEBRIS.

(b) MANGANESE K_α X-RAY MAP; 4.5×10^3 COUNTS.

Figure 12. - Scanning electron micrograph and energy dispersive X-ray analysis of wear debris of single-crystal manganese-zinc ferrite transferred to iron rider as result of five passes in high vacuum (10^{-8} N/m^2). Sliding velocity, 3 mm/min; temperature, 25° C.